The Nontidal Flow in the Providence River of Narragansett Bay: A Stochastic Approach to Estuarine Circulation

ROBERT H. WEISBERG

Graduate School of Oceanography, University of Rhode Island, Kingston 02881

(Manuscript received 22 January 1976, in revised form 12 April 1976)

ABSTRACT

Atmospherically driven flow in the Providence River (a partially mixed estuary) has been examined using a 51-day velocity record measured 2 m from the bottom. Velocity fluctuations at time scales between the steady-state gravitational convection and the tidal oscillations were large and almost exclusively wind-induced. The mean and variance of the velocity component lying along the channel axis were 11.7 cm s^{-1} (landward) and 166.9 $cm^2 s^{-2}$. Of this axial current variance 48% resided at subtidal frequencies as compared to 45% associated with semidiurnal tides (the remaining 7% was mostly due to higher tidal harmonics). Over the most energetic portion of the axial current spectrum (periodicities of 4–5 days), 97% of the variance was coherent with the wind velocity component lying along the direction of maximum fetch, with the current lagging the wind by about 4 h. Owing to this extremely high coherence, a linear time-invariant stochastic model reproduced the axial current from the two orthogonal wind velocity components to within an rms error of 2.3 cm s^{-1}. The wind also had a marked effect upon the density field. It is concluded that the effects of wind can permeate the entire water column of a partially mixed estuary and can be of equal (or greater) importance to the circulation as the tides or gravitational convection.

1. Introduction

Estuarine circulation is composed of both tidal and nontidal currents. Gravitational convection—one aspect of the nontidal portion—has been a topic of extensive research during the past few decades since it drives the two-layered mean flow normally associated with an estuary (e.g., see Cameron and Pritchard, 1963). Between the quasi-steady-state gravitational convection and the tidal oscillations there exists a broad range of time scales over which energetic motions may also occur. This paper examines the effects of wind and other atmospheric inputs on these intermediate scales of estuarine motion.

In contrast with gravitational convection there have been relatively few treatments of atmospherically driven estuarine flow. Pickard and Rodgers (1959) noticed a wind-induced shifting of the mean velocity profile in the Knight Inlet, British Columbia; Weisberg and Sturges (1976) found the nontidal circulation in the West Passage of Narragansett Bay, R. I., to be dominated by wind-induced fluctuations; and a steady-state analytic model by Hansen and Rattray (1965) implied that a small wind stress could change the circulation and density distribution due to gravitational convection alone. Other related papers include those of Bowden (1953) and Van Dorn (1953). Observations of wind effects on continental shelf and large lake circulations are more prevalent in recent literature. For example, Ketchem *et al.* (1951) observed storm-induced stratification changes in the New York Bight, Huyer and Pattulo (1972) found high wind and current coherence off the coast of Oregon, Cannon (1972) attributed current reversals in the Juan de Fuca Canyon to wind, and Csanady (1973) concluded that short bursts of wind are a primary source of motion in the Great Lakes.

The present paper will examine the effects that typical variations in wind velocity, atmospheric pressure and river inflow have on the nontidal flow in the Providence River section of Narragansett Bay, R. I. The partition of fluctuation kinetic energy will be discussed with respect to the various forcing mechanisms thus determining the inputs that must be included to adequately model the circulation or parts of it. The non-tidal flow will then be stochastically modeled by passing the appropriate inputs through time-invariant linear filters. A stochastic approach is used since the wind velocity may be characterized as a random function of time [see Papoulis (1965) for a general discussion of stochastic processes]. If we then postulate some coupling between the wind and water velocities, it is appropriate to determine an input-output relation, whereby, given the wind velocity (and any other important random or deterministic variates), we can estimate the current velocity. We will employ linear mean-square estimation to compute the filters. This results in an estimate based solely upon the data. As such, it is free of preconceived notions about the internal dynamics of the coupling.

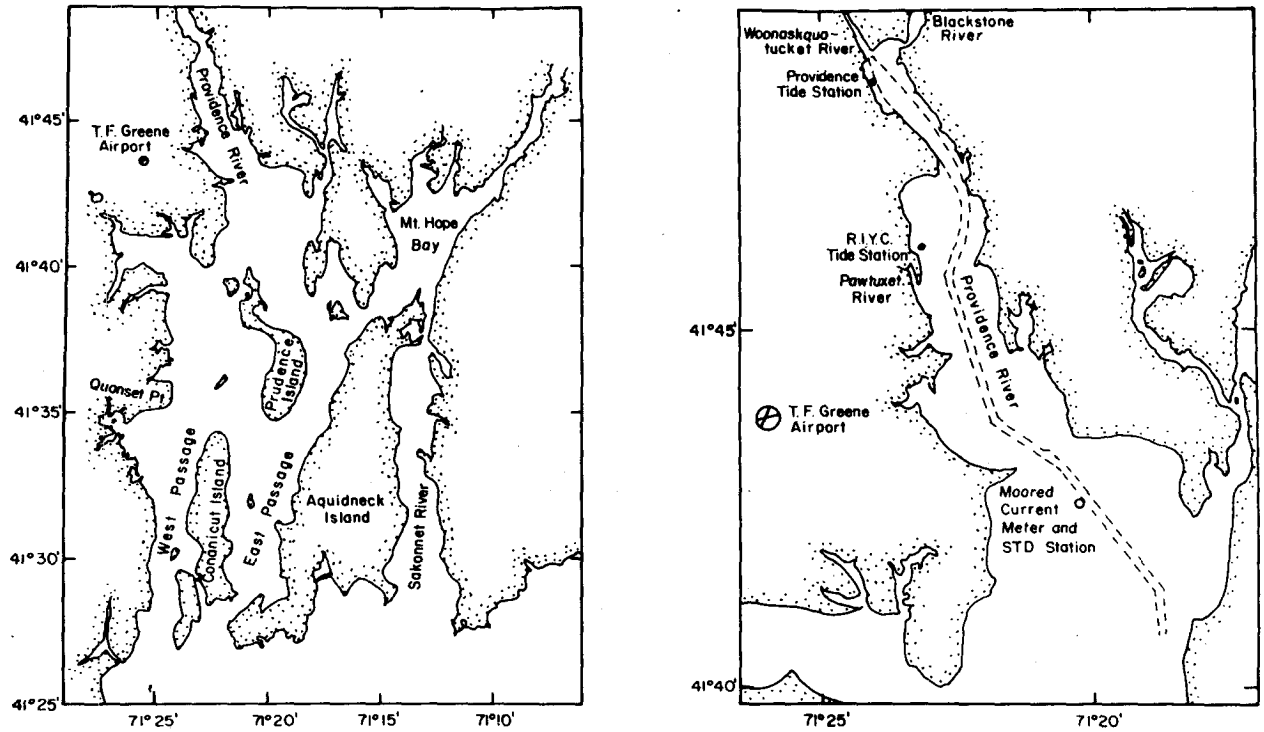

FIG. 1. Narragansett Bay, R. I., station locations are shown in the enlargement of the Providence River section. The dotted lines denote the channel in which the velocity and STD measurements were made.

A linear relationship between the wind and current velocities is suggested by empirical studies of momentum transfer across the air-sea interface. Wu (1968) has shown that the wind stress is proportional to the square of a boundary layer scaling velocity. If the wind stress is continuous and the boundary layer scaling is similar across the air-sea interface, then the wind-induced water speed should be proportional to the wind speed. These arguments were used by Wu (1973) to calculate a wind factor (the ratio of water speed to wind speed) from historical data.

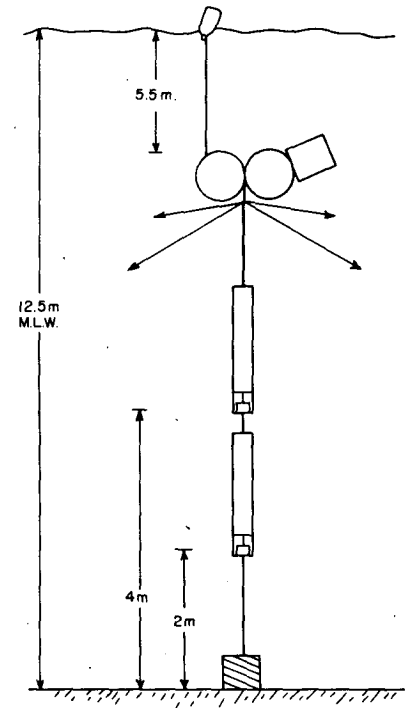

FIG. 2. The subsurface current meter mooring.

2. Field program and methods

The Providence River section of Narragansett Bay (Fig. 1) is a geometrically simple, partially mixed estuary, with a surface to bottom salinity differential of 2–3‰, a tidal height range of about 1 m, and a tidal current range of about 50 cm s^{-1}. Previous data pertaining to the density field and transport in the Providence River are available in Hicks (1959, 1963).

Currents and stratification were measured near the entrance to the Providence River in a fairly straight channel with a mean low water depth of 12.5 m. Two Geodyne model 850 current meters were buoyantly suspended at distances of 2 and 4 m off the bottom as shown in Fig. 2. They were in place from 18 October to 9 December, 1972. The instrument at 4 m failed but the other one gave an uninterrupted 51-day record of velocity.

Near-bottom as opposed to near-surface measurements were made to avoid data contamination by both mooring motion and the rectification of high-frequency surface-gravity-wave-induced motions. Letting the water column act as a high-frequency filter would not

have been suitable unless the signals of interest were allowed to pass through. Since an estuary is a semi-enclosed basin of limited storage capacity, motions at subtidal frequencies originating at the surface must be transmitted through the water column. Although the magnitude of the response at a given depth will depend upon stratification, continuity suggests that the near-bottom subtidal current fluctuations should be in the opposite direction from those at the surface.

The current meters sensed speed with a Savonius rotor and direction with a compass and vane. The sampling interval was 15 min within which 23 speed words of approximately 5 s duration were consecutively recorded on a magnetic tape. Corresponding to each

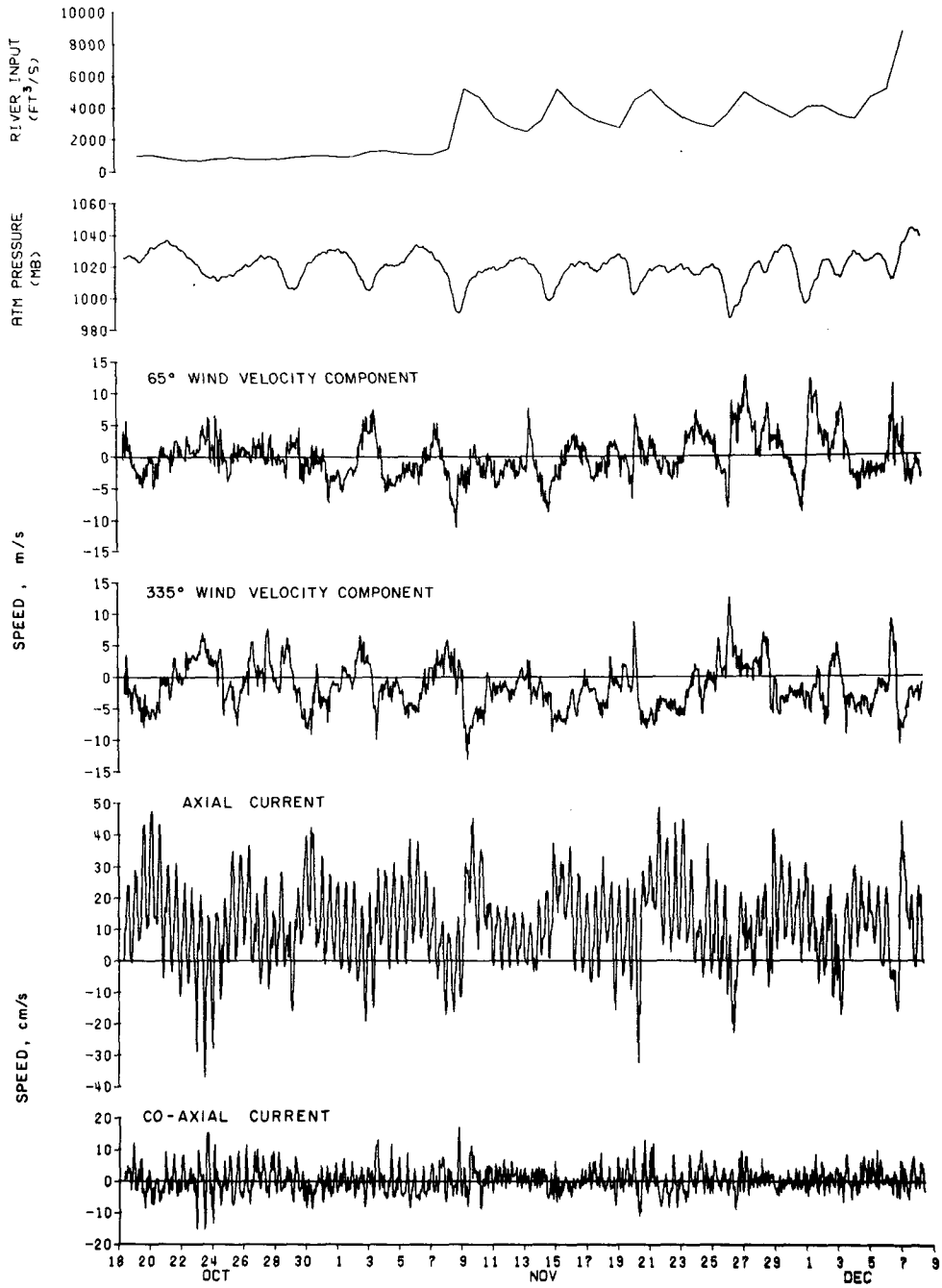

FIG. 3. The hourly vector averaged water velocity components, the discrete hourly wind velocity components, atmospheric pressure from the T. G. Green Airport weather station, and the daily mean river inflow.

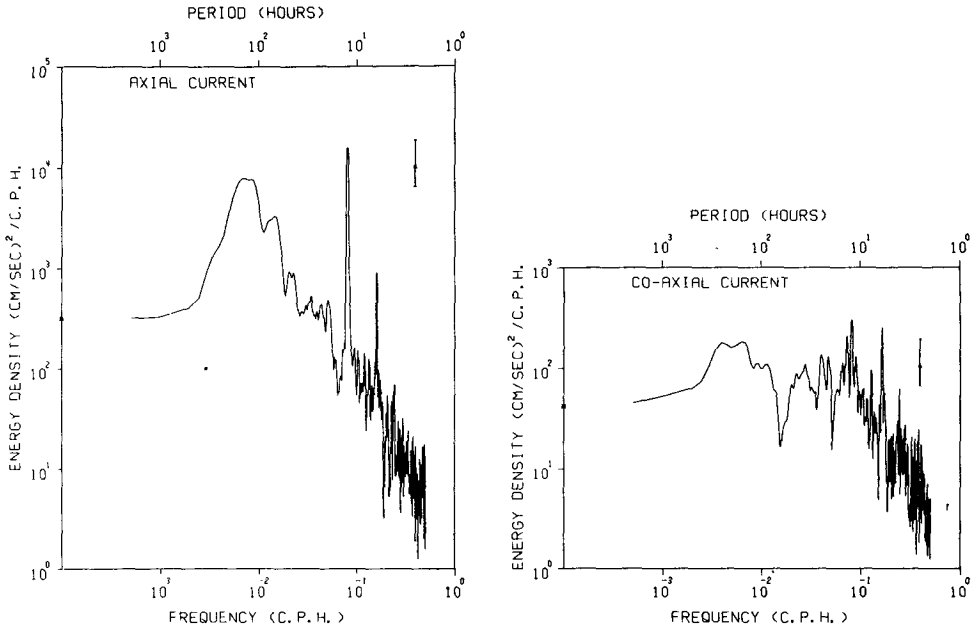

FIG. 4. The axial and co-axial current fluctuation kinetic energy density spectra. The 80% confidence interval based upon a chi-squared distribution with 12 degrees of freedom is given in the upper right corners.

speed word instantaneous compass and vane positions were also recorded. These were later formed in hourly vector averages.

Hourly values of wind speed and direction were obtained from the T. F. Green Airport weather station and the U. S. Naval Air Station at Quonset Point (Fig. 1). The energy distributions from the Green and and Quonset winds were equal to within 1% and their coherence was greater than 0.9 for periodicities longer than diurnal. For shorter periodicities their coherence dropped off. This suggested a low-frequency uniformity in the wind field (within a scale factor) so only the T. F. Green Airport wind data were used for subsequent analysis. Hourly values of atmospheric pressure corrected to mean sea level were also provided by the weather station.

Temperature and salinity were sampled for 83 consecutive hours at four depths using a Beckman model RS5-3 *in situ* salinometer. The National Ocean Survey, NOAA, assisted in the measurement of sea level at two stations along the Providence River and the U. S. Geological Survey provided daily mean flow rates for the Blackstone, Pawtuxet, Woonasquatucket and Mosshassuck rivers.

Standard time series analysis techniques have been employed. Although the computation details are excluded herein, they are available in Weisberg (1975) and in the references cited throughout the text. Similar methods have previously been applied to sea level analysis, e.g., Groves and Hannon (1968) and Wunsch (1972).

TABLE 1. The axial and co-axial component means and variances computed from a 51-day current meter record 2 m. from the bottom at the entrance to the Providence River section of Narragansett Bay.

	$\bar{u}$ (cm s^{-1})	$(\overline{u-\bar{u}})^2$ (cm^2 s^{-2})
Axial	11.7	166.9
Co-axial	0.2	16.1

3. The data

a. *Current observations*

Fig. 3 shows the hourly vector-averaged axial and coaxial velocity components, the raw hourly winds and atmospheric pressure, and the daily mean river inflow. The axial current is positive toward 320° (the channel axis) and the co-axial current is positive at a clockwise right angle to the channel axis. The co-axial current consists of semidiurnal and higher frequency oscillations. Its mean is near zero and subtidal fluctuations are small. The axial current, on the other hand, has a sizable mean value along with large subtidal and tidal oscillations. The axial and co-axial means and variances are summarized in Table 1.

The axial current mean, being steady and directed landward toward Providence, is consistent with the near-bottom mean flow characteristic of a partially mixed estuary driven by gravitational convection. The magnitude compared favorably with Hicks' (1959) estimate of 5 cm s^{-1} using mass conservation for an idealized two-layered flow.

One way of describing the axial and co-axial current variances is by their kinetic energy density spectra (Fig. 4). The values given differ from the kinetic energy of the velocity component fluctuations by the factor $\frac{1}{2}\rho$, where ρ is the water density. The axial current spectrum has significant peaks centered about periodicities of 4–5 days, semidiurnal and quarter diurnal, while the co-axial current spectrum is much flatter and roughly two orders of magnitude smaller. The low-frequency drop-off in the spectra contrast sharply with the characteristic monotonic rise observed in most deep ocean current spectra. This suggests a limitation in the low-frequency response of an estuary to external forcing. Since the flow is so strongly polarized along the channel axis we will limit our attention to the axial current.

A second way of viewing the velocity fluctuations is in terms of their kinetic energy distribution functions shown in Fig. 5. These are integrated and normalized spectral density functions giving the partition of the fluctuation kinetic energy into the various modes of flow. Table 2 summarizes the partition of the axial current variance. Roughly 48% of the fluctuation kinetic energy resides at subtidal frequencies. Excepting the very small amount associated with diurnal and fortnightly tides, this 48% is due to nontidal random forcing. Thus, estuarine models that neglect everything but tidal and mean flows may be far too oversimplified.

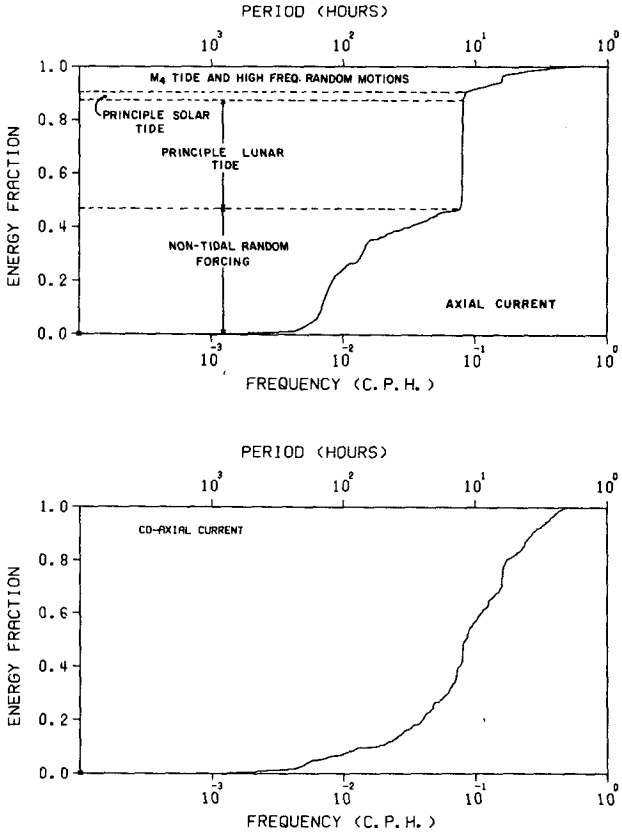

FIG. 5. The axial and co-axial fluctuation kinetic energy distributions.

TABLE 2. The partition of fluctuation kinetic energy for the axial component of current 2 m from the bottom at the entrance to the Providence River section of Narragansett Bay.

Constituent	Variance $(\overline{u-\bar{u}})^2$ (percent)
Nontidal random forcing	48
Principle lunar tide M_2	43
Principle solar tide S_2	2
Quarter diurnal tide M_4	2
M_6, surface seiches, and high-frequency noise	5

b. *Atmospherically induced velocity fluctuations*

The portion of the axial current variance at subtidal frequencies will not be viewed with respect to the various atmospheric inputs, particularly the wind. Since a description is being sought for direct coupling of the wind with the water, the sign convention used for the wind is the same as for the water, i.e., a 335° wind blows *toward* 335° and so on. The wind components of 335° and 65° shown in Fig. 3 were chosen by rotating the vector wind time series until an optimal coherence was obtained between one of its components and the axial current. This optimal coherence occurred along 335° which, as expected, corresponds to the direction of maximum fetch (see Fig. 1).

Fig. 6 presents the same time series as Fig. 3 after low-pass filtering to remove tidal and higher frequency oscillations (a 49 h Gaussian filter having a half-amplitude response of somewhat less than 2 days was used). The most striking feature is the mirror image correlation between the wind component blowing in the direction of maximum fetch and the axial current. This inverse relationship follows from continuity since the Providence River lacks the storage capacity for sustained nontidal transport, i.e., water being advected landward by wind drag on the sea surface must return seaward at depth and vice versa. The axial current does not appear to be correlated with the river input or atmospheric pressure.

The fact that the mean value of axial current did not respond to a factor of 2 change in river input midway through the experiment is not overly surprising. Gravitationally convected mean transport in a partially mixed esturay is generally 1–2 orders of magnitude larger than the river input and the effects of river input changes are buffered by corresponding stratification changes. Similar insensitivity to river input changes were found in the Patuxent River estuary by Cannon (1969).

The absence of any clear relation between the atmospheric pressure and velocity fluctuations is also

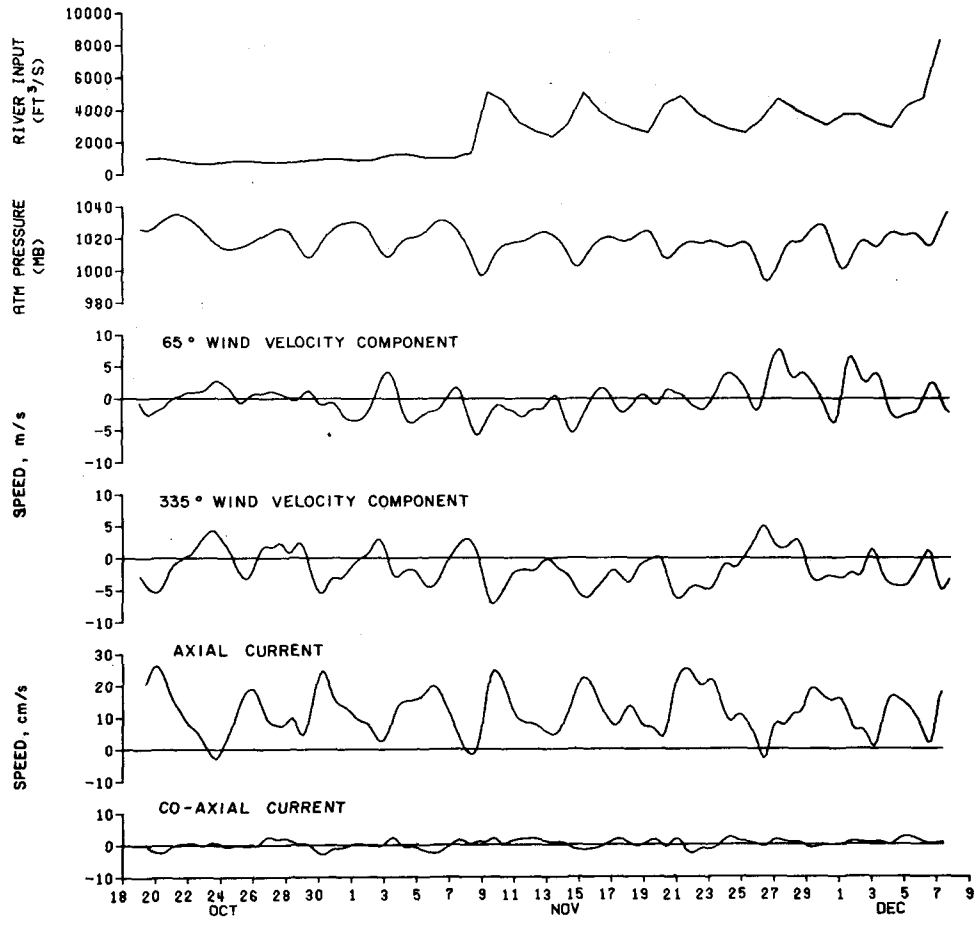

FIG. 6. Low-pass filtered versions of the time series in Fig. 3.

reasonable. The sea surface responds as an inverted barometer to atmospheric pressure by approximately 1 cm per millibar. Since the response is barotropic, an expression for the resulting speed may be derived from the continuity equation

$$U_P = K\frac{L}{H}\frac{\partial p_a}{\partial t}, \tag{1}$$

where L and H are the lengths and depths of the channel, K is a proportionality constant equal to 1 cm mb^{-1}, P_a the atmospheric pressure, and U_P the speed induced by its change. Putting in the appropriate numbers yields a velocity on the order of tenths of a centimeter per second. Thus, except during extreme storm events, a correlation between nontidal flow and atmospheric pressure is not expected.

c. *Sea level*

The residual sea level corrected for the inverse barometer effect of atmospheric pressure responded by a few centimeters to fluctuations in wind stress. However, the overall correlation between residual sea level and wind stress was poor [the data are shown in Weisberg (1975)]. This suggests that when trying to relate water transport to atmospheric inputs in an esturay or embayment, direct velocity measurements, although more difficult to obtain, are much more appropriate than sea level measurements. Comparing the amplitudes of residual sea level and nontidal current fluctuations to their background noise (the tides) shows that the signal-to-noise ratio is of order 10^{-2} for residual sea level and of order unity for the nontidal current. Not only is the signal-to-noise ratio small for residual sea level but there are physical reasons for the presence of noise such as directionally varying bottom slopes and shoreline irregularities.

d. *Stratification*

The purpose of the 83 consecutive hour temperature and salinity observations was to relate temperal variations in the water column to the nontidal transport. Salinity was the limiting factor in the measurement precision with a scatter of roughly 0.2‰. Since both salinity and temperature varied over the water column, their relative contributions to σ_t are important. The temperature-salinity correlation was strong with the

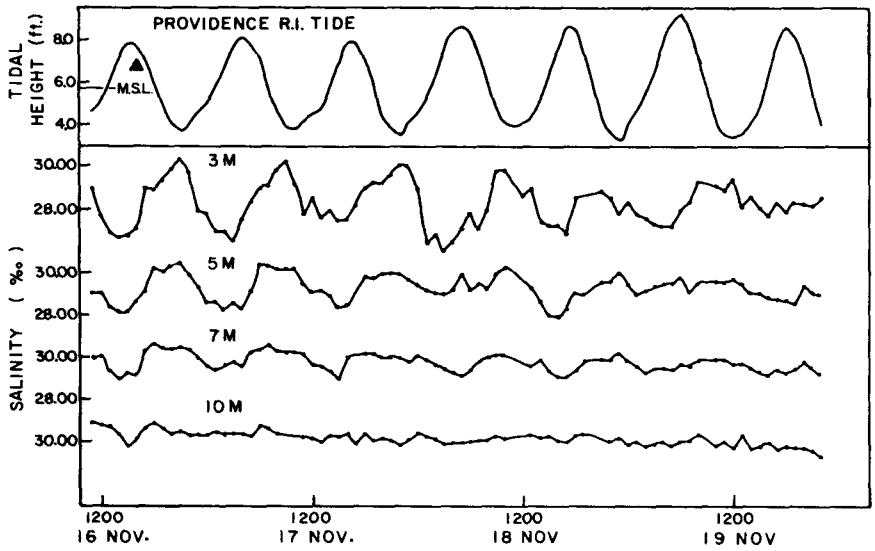

FIG. 7. Salinity (density) time series at four discrete levels near the current meter mooring and tidal height at Providence.

surface waters being cooler and fresher than the bottom waters. The maximum vertical temperature and corresponding salinity differences were 1.7°C and 3.5‰ which, when transformed to σ_t units, yield 0.27 and 2.72, respectively. The minimum vertical temperature and corresponding salinity differences were 0.2°C and 0.5‰, or 0.03 and 0.40 σ_t units. Therefore, salinity accounted for 90% of the density fluctuations.

Time series of salinity at the four discrete depths along with the corresponding tidal height curve from Providence are given in Fig. 7. Note that the tidal variations in salinity (density) are 180° out of phase with the tidal height, i.e., high salinity occurs at low water. This is an anomalous behavior for an estuary in which the salinity should increase to seaward at all depths. The anomaly is not of tidal origin as there are no nodes within Narragansett Bay. Since the magnitudes of the low-water surface salinity and temperature are similar to their respective magnitudes at the bottom, the origin of the anomaly appears to be from the bottom via upwelling. The anomaly persists throughout the record with a decay only noticeable over the last day.

Upwelling is kinematically consistent with the simultaneous wind and current observations. Prior to the STD measurements the wind blew seaward for about 2.5 days, tending to drive the surface water out of the Providence River. The corresponding nontidal near-bottom flow had a landward component sufficiently above the mean value to cause a relatively salty dome of water landward of the measurement site. What is observed, therefore, appears to be the tidal oscillations of the dome about the measurement site. Since the dome is intrinsically unstable in the absence of wind stress, it would be expected to propagate its energy seaward as an internal seiche as well as being advected by the nontidal flow. Relaxation as an internal seiche would yield a decay time of less than a day which is consistent with the wind and salinity observations.

4. The models

The data suggest that under typical conditions oscillations at subtidal frequencies comprise a large portion of the circulation within a partially mixed estuary (Tables 1 and 2), and that these oscillations seem exclusively wind-induced. Thus only the wind need be included in modeling the subtidal velocity fluctuations. Fig. 8 shows the kinetic energy densities for the wind components and Fig. 9 gives their corresponding distributions. The similarity between the low-frequency portion of the axial current spectrum and the 335° wind spectrum is quite evident, while the 65° wind spectrum bears little resemblance to the axial current spectrum. Therefore, the linear relationship between the 335° wind component and axial current will be examined first, after which the 65° wind component will be added.

a. The mean plus the 335° wind velocity component

We will consider a linear system wherein the nontidal axial current is given by the sum of a mean value (presumably due to gravitational convection), subtidal fluctuations related to the maximum fetch wind velocity component, and extraneous noise. The system is modeled by the equation

$$y(t)=\bar{y}+\int_{-\infty}^{\infty} h(\tau)x(t-\tau)d\tau+\epsilon(t)$$
$$=\hat{y}(t)+\epsilon(t), \qquad (2)$$

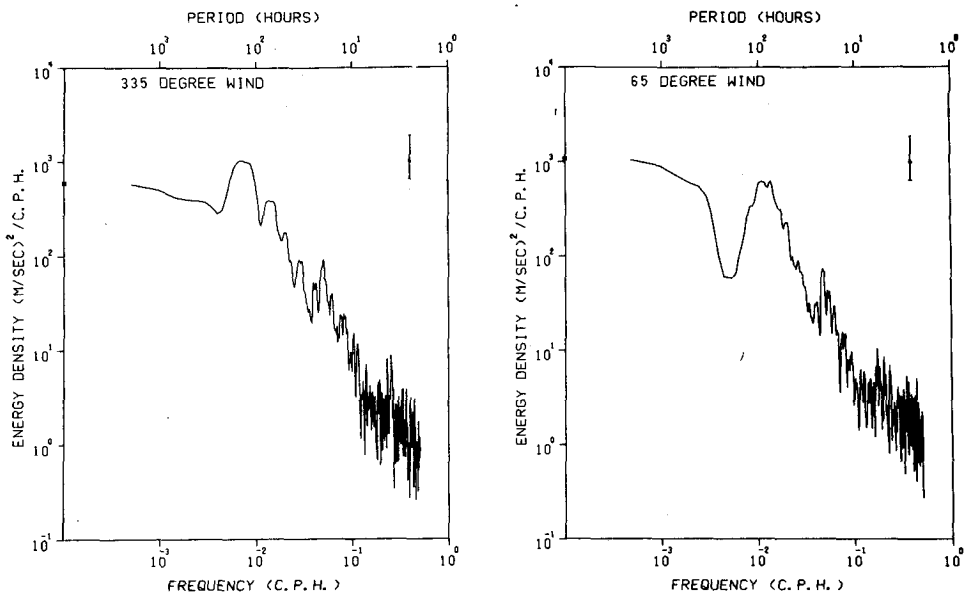

FIG. 8. The 335° and 65° wind velocity component fluctuation energy density spectra. The 80% confidence interval based upon a chi-squared distribution with 12 degrees of freedom is given in the upper right corners.

where $y(t)$ is the observed axial current, $\hat{y}(t)$ the axial current estimated from the mean $\bar{y}$ plus the 335° wind velocity component $x(t)$, and $\epsilon(t)$ is the extraneous noise. The system's response to the wind forcing is given as a convolution between an impulse response function $h(\tau)$ and $x(t)$. The response is assumed to be time-invariant and is characterized in the frequency domain by a transfer function $H(f)$; $H(f)$ and $h(\tau)$ are Fourier transform pairs. They are calculated in a manner which minimizes the mean-square error between the observed axial current $y(t)$ and the estimated axial current $\hat{y}(t)$ [e.g., see Bendat and Piersol (1971) or Papoulis (1965)].

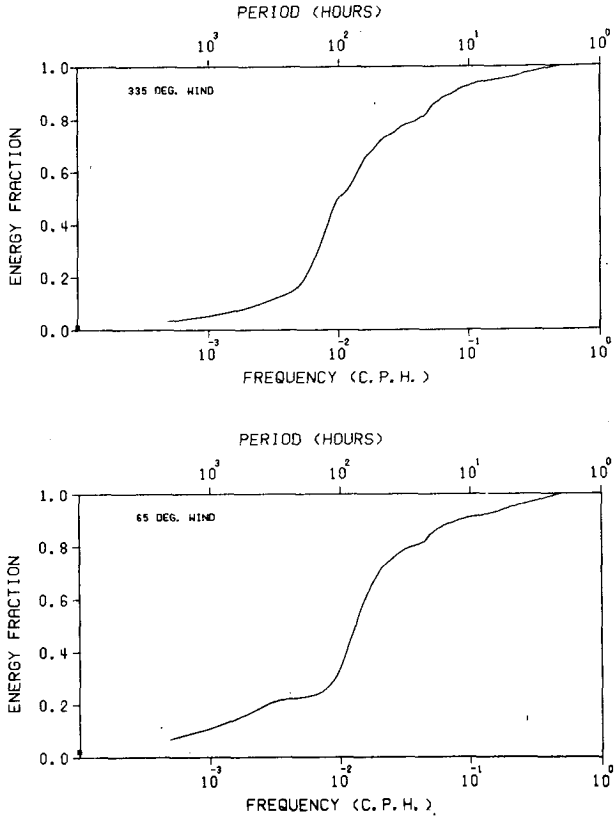

FIG. 9. The 335° and 65° wind velocity component fluctuation kinetic energy distributions.

The linear relation between $x(t)$ and $y(t)$ is described by the ordinary squared coherence and transfer functions. The first is a real function, varying from zero to one, expressing the fraction of output energy which may be accounted for by a linear operation upon the input. The second is a complex quantity giving the amplitude and phase of the response for the *coherent* portion of the wind and current spectra.

The ordinary squared coherence between the 335° wind velocity component and the axial current is shown in Fig. 10. The coherence is high for periodicities between 10 days and 16 h. Over the most energetic portion of the spectrum (periodicities of 4–5 days) as much as 97% of the axial current variance may be accounted for by the component of wind along the direction of maximum fetch. The coherence drops off for periods longer than 10 days or shorter than 16 h and there is also a dip about 24 h due to the deterministic tide. The low-frequency drop-off (to be discussed later) may be attributed to stratification and the wind energy distribution. The high-frequency drop-off corresponds to the presence of tidal oscillations

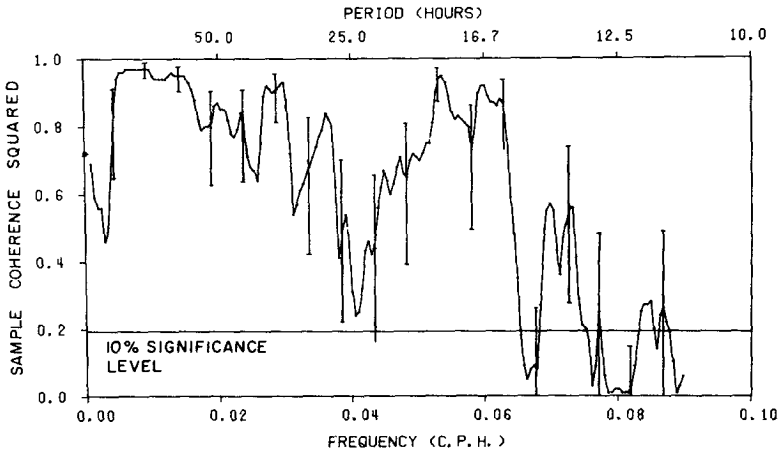

FIG. 10. The ordinary squared coherence between the 335° wind velocity component and the axial current. The 10% significance level and 90% confidence intervals for random errors are from Amos and Koopmans (1963) tables with 12 degrees of freedom.

and the absence of appreciable wind forcing (less than 10% of the wind energy resided at periods <16 h).

The amplitude and phase shift for the response is shown in Fig. 11. Within the confidence intervals, the ratio of water speed to wind speed is fairly uniform at 2–3 (cm m^{-1}) for periodicities of 10 days to 16 h. The amplitude drops off rapidly at longer periodicities indicating that the water column cannot respond well to very-low-frequency forcing. It tails off slowly at shorter periods and becomes noisy indicating that the coherent portion of the spectrum is responsive but that the signal-to-noise ratio is greatly reduced. The phase shift is also fairly uniform. Within the confidence intervals the axial current lags the wind by about 4 h. This lag is consistent with the time required to transfer momentum through the water column.

The frequency domain description of the model is summarized by Fig. 12 in which the axial current spectrum estimated from the 335° wind component is compared with the actual observed axial current spectrum. The estimated and observed spectra agree extremely well for periodicities larger than 16 h. Shorter time scales have been excluded since the spectra diverge.

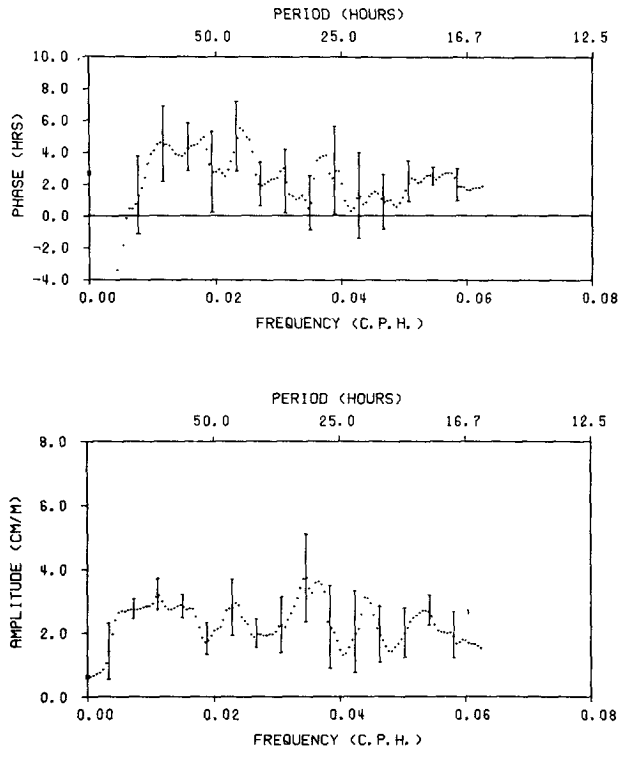

FIG. 11. The transfer function amplitude (bottom) and phase (top) between the 335° wind velocity component and the axial current. The 80% confidence intervals were calculated as outlined in Bendat and Piersol (1971) using 12 degrees of freedom.

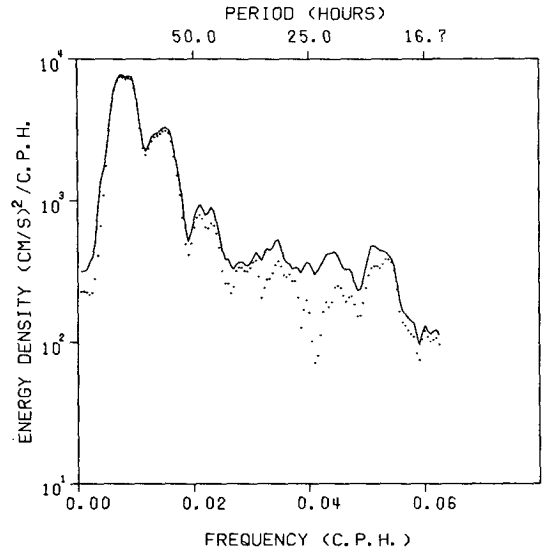

FIG. 12. The observed axial current spectrum and the portion of it which is coherent with the 335° wind velocity component.

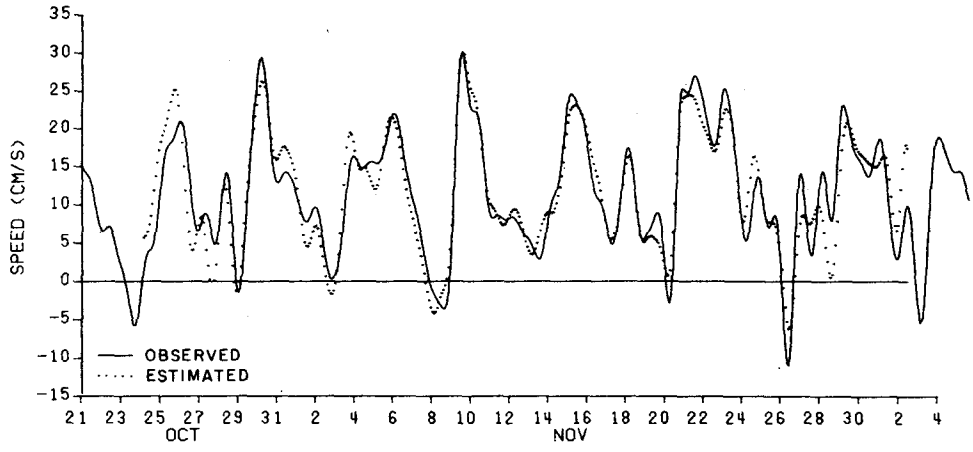

FIG. 13. The observed nontidal axial current (solid line) compared with its estimate (dotted line) based upon the 335° wind velocity component.

Periodicities <16 h were similarly excluded in the time domain estimation. $H(f)$ was smoothly tapered to zero using a half-cosine bell between periodicities of 40 and 16 h. Lower frequencies were left unweighted, while higher frequency estimates were set equal to zero. The tapering and high-frequency exclusion resulted in a total nontidal information loss of roughly 10%. The impulse response function, or linear mean-square-estimation filter, was obtained by Fourier transforming the tapered $H(f)$ and the nontidal axial current was then estimated using Eq. (2). Fig. 13 compares the estimated and observed nontidal axial currents, the observed axial current having been low-pass filtered with a response function having the same taper as above. The two agree extremely well suggesting that a linear parameterization of the wind/current coupling is very useful. The lack of estimation data at the ends is a consequence of finite filter length.

b. *The mean plus the 335° and the 65° wind velocity components*

The nontidal axial current estimation may be improved by adding the second wind component. Along with the mean value we now have two correlated inputs, $x_1(t)$ and $x_2(t)$, the 335° and 65° wind velocity components, respectively. The system is modeled by the equation

$$y(t)=\bar{y}+\int_{-\infty}^{\infty} h_1(\tau)x_1(t-\tau)d\tau + \int_{-\infty}^{\infty} h_2(\tau)x_2(t-\tau)d\tau+\epsilon(t)$$
$$=\hat{y}(t)+\epsilon(t), \qquad (3)$$

where the terms have the same definitions as before. The response is again assumed to be time-invariant. $H_1(f)$ and $h_1(\tau)$ are the transfer function and impulse response function for the 335° wind velocity component; $H_2(f)$ and $h_2(\tau)$ are the counterparts for the 65° wind velocity component and they are calculated in a manner that minimizes the mean-square error between the observed axial current $y(t)$ and the estimated axial current $\hat{y}(t)$ (e.g., Bendat and Piersol, 1971).

The reasons for adding the 65° wind component are twofold. First, since Narragansett Bay widens and then branches into two separate passages south of the measurement location, one might expect that the effects of 65° wind component would be coupled to the Providence River by causing motion south of it. Second, any unaccounted for inputs show up as extraneous noise at the output. Therefore, by including the 65° wind component the extraneous noise due to it is reduced. This is evident in Fig. 14 which shows the partial squared coherence computed between the residual 335° wind velocity component and axial current variables after removing the influence of the 65° wind component from both. The values of the partial squared coherence are slightly higher than for the ordinary coherence shown previously.

If, rather than subtracting the effects of the 65° wind component, they are incorporated in the analysis, then a third measure of coherence results. The multiple-squared coherence shown in Fig. 15 gives the total amount of the axial current variance accountable for by linear relationships with both orthogonal wind components.

The linear mean-square estimation based upon the total wind and the mean axial current was computed in a similar manner as before. The transfer functions were tapered to zero and their respective impulse response functions were obtained via inverse Fourier transformation. Convolutions were then performed on the 335° and 65° wind velocity components and the resulting time series were summed along with the mean axial current to give the estimated axial current. Fig. 16 compares the estimated and observed nontidal axial currents. Improvement over Fig. 13 is seen in both the closure of the curves and the phase locking.

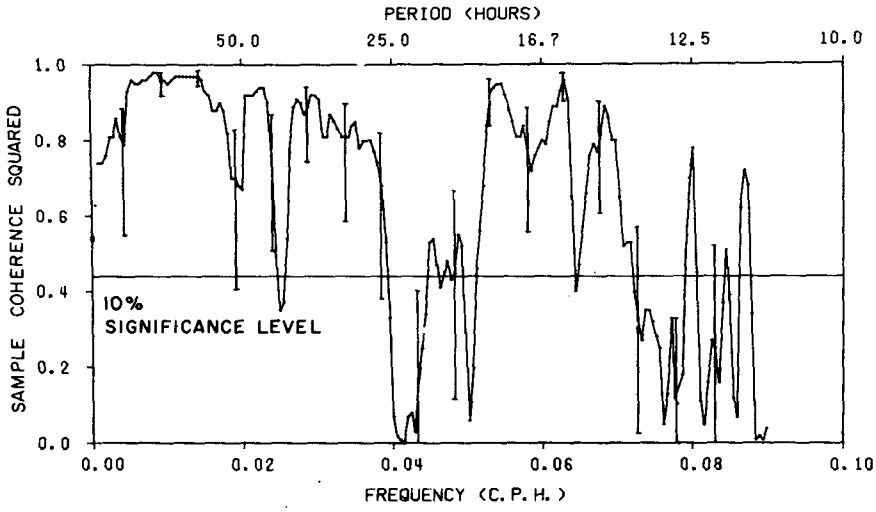

FIG. 14. The partial squared coherence between the 335° wind velocity component and the axial current after removing the influence of the 65° wind velocity component. The 10% significance level for random errors is from Groves and Hannan (1968) and the 90% confidence intervals for random errors are from Amos and Koopmans (1963) using 11 degrees of freedom.

c. Root-mean-square errors

Three linear mean-square estimation models have now been presented: 1) the mean axial current alone (implicit in Tables 1 and 2), 2) the mean axial current plus the effects of the wind component along the direction of maximum fetch, and 3) the mean axial current plus the effects of both orthogonal wind components. These may be summarized by comparing their mean-square errors. Papoulis (1965, p. 405) shows that the mean-square estimation error may be computed by summing the residual spectrum. Miyata and Groves (1971) point out, however, that the residual spectrum is a biased estimate. To remove the largest source of the bias they suggest that the residual spectrum be multiplied by the factor $\nu/(\nu-2p)$, where ν is the number of degrees of freedom for the individual spectral estimates and p the number of inputs (not including the mean). This factor has the values of 1.0, 1.2 and 1.5, respectively, for the three cases presented. Table 3 gives the resulting mean-square (ms) estimation errors corrected for bias and their positive square roots (rms errors). The final model accounts for the observations to within an rms error of 2.3 cm s^{-1}.

5. Discussion

a. Model interpretation

The output of the final model is an optimal linear estimation of the nontidal flow at a point in the Providence River based upon a mean value and concurrent wind velocity observations. It is optimal in the sense

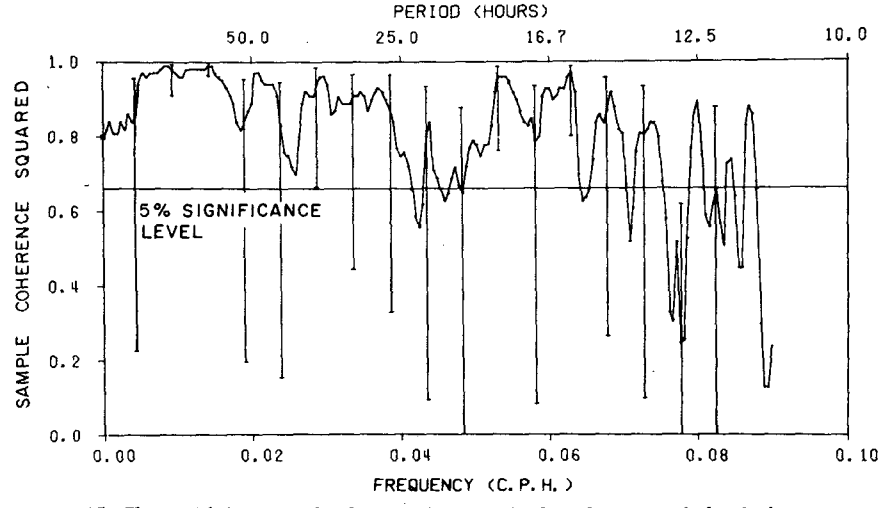

FIG. 15. The multiple-squared coherence between both orthogonal wind velocity components and the axial current. The 5% significance level and 95% confidence intervals for random errors are from Groves and Hannan (1968) using 12 degrees of freedom.

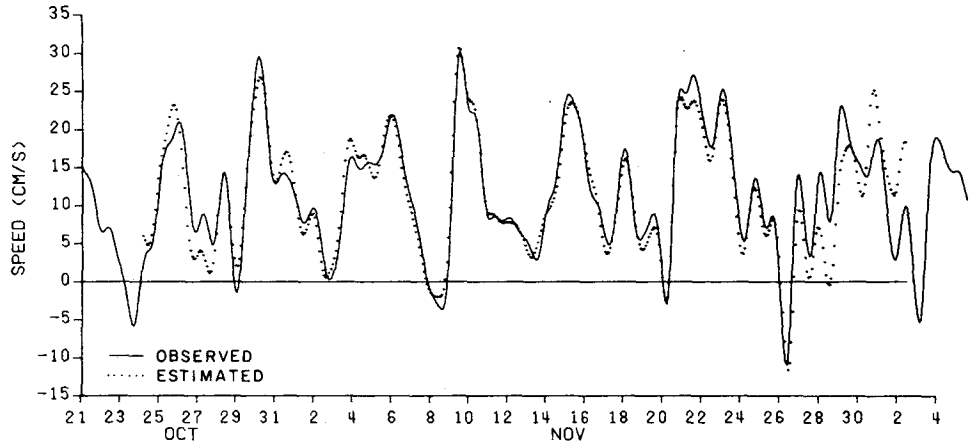

FIG. 16. As in Fig. 13 based upon both orthogonal wind velocity components.

that the estimation error is orthogonal to the wind data used in forming the estimate (the orthogonality principle of linear mean-square estimation). Simply stated, only the portion of the axial current which is coherent with the wind can be modeled; incoherent events cannot. Thus, circular reasoning objections stemming from the use of the same time series to compute the transfer functions and perform the estimation do not apply and the accuracy of the model (Fig. 16) is merely a reflection of the strong correlation between the wind and current.

The confidence limits for random errors assigned to the transfer function and coherence estimates are properties of the present data. They should also apply to future data at the same location if the model is unbiased and the assumptions are valid, i.e., time invariance, linearity, and (to a lesser extent) that the variable distributions are Gaussian. There are many sources of bias errors, some of which have already been mentioned and corrected for. The more preplexing sources still remaining are the limited record length from which the spectral estimates were computed and the assumption of time-invariance. Record length limitations are particularly critical when studying certain geophysical phenomena where a preponderance of the energy is at low frequency. Resolution then becomes a problem. Averaging over a large enough frequency band relative to the record length in order to decrease random errors may result in biased spectral estimates if the spectrum is not uniform. Fortunately, the response of the subtidal current fluctuations to the wind was fairly uniform over the frequency range of interest.

Perhaps the most tenuous assumption then is time-invariance. If the real response changed, for example, due to seasonal changes in the stratification and horizontal density gradients, then the ouptut of the model would be biased up or down depending on the sign of the change. The model would also be biased with respect to any seasonal variation in the mean flow.

Departures from the linear and Gaussian assumption should be of little consequence. Whether or not the processes are strictly linear, the model still gives the best estimate in a minimum mean-square error sense. If the data were not strictly Gaussian, Amos and Koopmans (1963) suggest that the confidence intervals would not be altered by much.

The computational procedure did provide some check on the above error sources. A Hanning window was applied to the wind and current time series prior to computing the transfer functions. The estimation, however, was performed using the original hourly wind time series. Since a Hanning window weights the middle of the record more than the ends, considerably different data were used to compute the estimators than to compute the estimates.

What has been offered, then, is an optimal estimation based upon existing data. Arguments have been presented suggesting that the model should also apply fairly well to future data at the same location if the response remained stationary. However, this is an assumption to be viewed with caution because of unknown seasonal variability.

TABLE 3. The ms and rms errors associated with the estimated nontidal axial current based upon the mean alone, the mean plus the component of wind lying along the direction of maximum fetch (335°), and the mean plus both orthogonal wind components (335° and 65°).

Inputs	ms error $(\text{cm s}^{-1})^2$	rms error (cm s^{-1})
The mean axial current (from Tables 1 and 2)	80.2	9.0
The mean axial current plus the 335° wind component	7.8	2.8
The mean axial current plus both orthogonal wind components	5.2	2.3

b. Response characteristics

The response of the axial current to wind was uniform in between high- and low-frequency cutoffs. Factors affecting the high-frequency cutoff are the presence of tides, the absence of appreciable wind energy and the water's inertia. The uniformity of the response may have been due to the large observed variations in the density field tending to smooth over resonant internal modes. The low-frequency cutoff will now be examined further.

As a wind blows over an estuary, a small surface slope forms to balance the wind stress. The time required to start the water column in motion and redistribute enough mass to set up this slope is on the order of a few hours; afterward, the circulation must be closed with a return flow at depth equal to the downwind transport. For this closed circulation to continue, either mixing or isopycnal surface-level changes must occur. Either case requires work, so a criterion for the response of an estuary to wind may be derived by equating the energy required to sustain the responsive state versus the energy available to excite a response.

The potential energy (PE) associated with a change in density $\Delta\rho$ within a unit water column equals the integral of $\Delta\rho gz$ over the depth range η that the response extends. Consider a control volume with upstream and downstream cross sections a and b. If we neglect bottom friction and kinetic energy flux, then the flux of PE out of the control volume must equal the rate of working by the wind stress upon the free surface, or

$$\int_a (\Delta\rho_a gz)\mathbf{U}_f\cdot d\mathbf{s}+\int_b (\Delta\rho_b gz)\mathbf{U}_f\cdot d\mathbf{s}=\int_{\substack{\text{Free}\\ \text{surface}}} \boldsymbol{\tau}\cdot\mathbf{u}\,ds, \quad (4)$$

where $\mathbf{U}_f$ is the sectional mean river flow rate, $\mathbf{u}$ the wind-induced surface velocity, and $\boldsymbol{\tau}$ the wind stress. Assuming lateral homogeneity Eq. (4) becomes

$$\mathbf{U}_f\,\mathrm{PE_{Mix}}=\tau u L, \quad (5)$$

where

$$\mathrm{PE_{Mix}}=\int_0^{\eta}(\Delta\rho_a-\Delta\rho_b)gz\,dz. \quad (6)$$

The response has a characteristic time scale

$$T=\frac{\Delta\mathrm{PE_{Mix}}}{\tau u}=\frac{L}{U_f}, \quad (7)$$

i.e., the ratio of the energy required for the response to the rate at which energy is supplied by the wind is related to the sectional mean advection. If the wind can supply enough energy within this advective time scale then the response can be sustained.

Following Turner (1969), the rate of working by the wind stress upon the sea surface may be written as

$$\tau u=c_d\rho_a c_f W^3, \quad (8)$$

TABLE 4. Sample calculations of the wind speed required to sustain a full response in the Providence River.

	U_f (cm s^{-1})	$\mathrm{PE_{Mix}}$ (ergs cm^2)	W (m s^{-1})
Fall	0.4	1.2×10^5	~2
Spring	1.4	4.4×10^5	~4

where c_d is a drag coefficient, ρ_a the air density and c_f is the wind factor. Typical values for these constants in cgs units are $1\text{–}2\times10^{-3}$, $1\text{–}2\times10^{-2}$ and $1\text{–}2\times10^{-3}$, respectively, e.g., see Wu (1968, 1973). Using a conservative value for the lumped constant of order 10^{-8}, a criterion for sustained wind-induced flow follows from Eq. 5, i.e.,

$$W\geqslant(U_f\,\mathrm{PE_{Mix}}/10^{-8}L)^{\frac{1}{3}}. \quad (9)$$

Although crude, the assumptions underlying this response criterion would cause W to err as an underestimate so it should provide a base line for causality.

Table 4 gives estimates of the wind speed required to sustain a response over the entire water column in the Providence River during the fall and spring (minimum and maximum river runoff). $\Delta\mathrm{PE_{Mix}}$ was calculated using data from two stations in the Providence River separated by 5 km from Hicks (1963). The fall estimates agree with the observations. Recall (Fig. 9) that less than 17% of the total wind variance, or 4 m^2 s^{-2}, occurred at time scales longer than 10 days and since the corresponding energy density was small a full response could not be promoted at longer time scales. On the other hand, about 40%, or 9.7 m^2 s^{-2}, of the total wind variance was concentrated over periodicities of 4–5 days. Thus, rms wind speeds of well over 2 m s^{-1} were sustained over this energetic portion of the spectrum, consonant with the observed response.

The analysis suggests that the low-frequency response of a partially mixed estuary is determined by stratification, river runoff and the wind energy distribution. Therefore, the magnitude and the depth to which the response extends should vary seasonally. The wind energy distribution is probably the most important factor of the three and if the wind blew hard and long enough, a response over the entire water column would be expected irrespective of the other two.

6. Summary and conclusions

Velocity fluctuations occurring in a partially mixed estuary at time scales between the steady-state gravitational convection and the tidal oscillations have been examined using a 51-day velocity record 2 m from the bottom in the Providence River, R. I. The mean speed along the channel axis was steady and landward at 11.7 cm s^{-1}. The total axial current variance was 166.9 cm^2 s^{-2}, 48% of which resided at subtidal frequencies as compared to 45% in the semidiurnal tide.

Over the most energetic portion of the axial current spectrum (4–5 day periodicities), 97% of the variance was coherent with the wind velocity component along the direction of maximum fetch with the current lagging the wind by about 4 h. River runoff and atmospheric pressure were ineffectual in exciting an axial current response in the present study; however, they should be important during extreme storm events.

The coupling between the wind and water velocities was viewed as a stochastic process and linear mean-square estimation was used to model the axial current from its mean value and the two orthogonal wind velocity components. The model estimate agreed extremely well with the observations (Fig. 16).

Along with wind-induced water transport there also occurs upwelling (or downwelling) which is capable of redistributing mass over the entire water column. This phenomena was clearly observed in an 83 h sampling of salinity and temperature at four discrete levels, and the work performed by the wind stress on the estuarine surface was shown to be of sufficient magnitude to sustain the resulting density state.

The relationship between the residual sea level and the wind stress was examined. Due to a low signal-to-noise ratio, the residual sea level is a very poor indicator of nontidal estuarine flow. This result is in contrast to recent continental shelf findings (e.g., Cragg and Sturges, 1974), where geostrophy, increased fetch and elimination of local topographical effects all tend to enhance the signal.

In conclusion wind-induced motions can permeate the entire water column of a partially mixed estuary and can comprise an equal, if not larger, portion of the total circulation than tidal currents or gravitational convection. Exclusion of the wind in modeling either the nontidal (time-averaged) or instantaneous estuarine circulation could therefore result in significant errors. Stochastic modeling, as applied herein, is probably the most accurate way to estimate wind-induced motions at a point; however, it would be desirable to extrapolate the estimation over the entire water body. It seems appropriate to combine stochastic with numerical modeling; the stochastic portion, for example, could be a time-dependent boundary condition. The effects of seasonal variations on the general response characteristics of an estuary also requires further observation and analysis.

Acknowledgments. This research was sponsored in part by a University of Rhode Island Sea Grant, Project R/ES-5. I had many valuable discussions with Drs. J. Knauss, L. Leblanc and P. Richardson during the course of the work and preparation of the manuscript. Drs. W. Sturges and K. Kenyon helped in motivating my original interest in the topic. Mr. W. Kramer assisted with the computer graphics.

REFERENCES

Amos, D. E., and L. H. Koopmans, 1963: Table of the distribution of the coefficient of coherence for stationary bivariate Gaussian processes. National Technical Information Service, U. S. Department of Commerce.

Bendat, J. S., and A. G. Piersol, 1971: *Random Data: Analysis and Measurement Procedures*. Wiley-Interscience, 407 pp.

Bowden, K. F., 1953: A note on wind drift in a channel in the presence of tidal currents. *Proc. Roy. Soc.*, London, **A219**, 426–446.

Cameron, W. M., and D. W. Pritchard, 1963: Estuaries. *The Sea*, Vol. 2, M. N. Hill, Ed., Wiley, 306–324.

Cannon, G. A., 1969: Observations of motion at intermediate and large scales in a coastal plain estuary. Chesapeake Bay Institute, Tech. Rep. No. 52, 114 pp.

——, 1972: Wind effects on currents observed in Juan de Fuca submarine canyon. *J. Phys. Oceanogr.*, **2**, 281–285.

Cragg, J. A., and W. Sturges, 1974: Wind-induced currents and sea surface slopes in the eastern Gulf of Mexico. *Trans. Amer. Geophys. Union*, **55**, 283 (abstract).

Csanady, G. T., 1973: Wind-induced barotropic motions in long lakes. *J. Phys. Oceanogr.*, **3**, 429–438.

Groves, G. W., and E. J. Hannan, 1968: Time series regression of sea level on weather. *Rev. Geophys.*, **6**, 129–174.

Hansen, D. V., and M. Rattray, 1965: Gravitational circulation in straits and estuaries. *J. Marine Res.*, **23**, 104–122.

Hicks, S. D., 1959: The physical oceanography of Narragansett Bay. *Limnol. Oceanogr.*, **4**, 316–327.

——, 1963: Physical oceanographic studies of Narragansett Bay. *U. S. Fish Wildlife Ser. Spec. Sci. Rep. Fish.*, No. 457.

Huyer, A., and J. G. Pattullo, 1972: A comparison between wind and current observations over the continental shelf off Oregon, summer 1969. *J. Geophys. Res.*, **77**, 3215–3220.

Ketchum, B. H., A. C. Redfield and J. C. Ayers, 1951: The oceanography of the New York bight. *Pap. Phys. Oceanogr. Meteor.*, **8**, 1–46.

Miyata, M., and G. W. Groves, 1971: A study of the effects of local and distant weather on sea level in Hawaii. *J. Phys. Oceanogr.*, **1**, 203–213.

Papoulis, A., 1965: *Probability, Random Variables, and Stochastic Processes*. McGraw-Hill, 583 pp.

Pickard, G. L., and K. Rodgers, 1959: Current measurements in Knight Inlet, British Columbia. *J. Fish. Res. Bd. Can.*, **16**, 635–684.

Turner, J. S., 1969: A note on wind mixing at the seasonal thermocline. *Deep-Sea Res.*, **16**, Suppl., 297–300.

Weisberg, R. H., 1975: The non-tidal flow in the providence River of Narragansett Bay: A stochastic approach to estuarine circulation. Ph.D. thesis, University of Rhode Island, 127 pp.

——, and W. Sturges, 1976: Velocity observations in the west passage of Narragansett Bay: A partially mixed estuary. *J. Phys. Oceanogr.*, **6**, 345–354.

Van Dorn, W. G., 1953: Wind stress on an artificial pond. *J. Marine Res.*, **12**, 249–276.

Wu, J., 1968: Froude number scaling of wind stress coefficient—A correlation of wind stresses determined at all fetches. Tech. Rep., Hydronautices Inc., Laurel, Md., 67 pp.

——, 1973: Prediction of near surface drift currents from wind velocity. *J. Hydraulics Div., ASCE*, **99**, 1291–3101.

Wunsch, C., 1972: Bermuda sea level in relation to tides, weather, and baroclinic fluctuations. *Rev. Geophys. Space Phys.*, **10**, 1–49.